Expanded View Figures

Figure EV1. ER-phagy receptors involvement in delivery of ATZ_{NNN} polymers to endolysosomal compartments.

A Control of genetic *Fam134B*-, *Sec62*-, and *Tex264*-KO, respectively. * shows a non-specific cross-reaction of the antibody.

B Same as Fig 2A in cells edited with CRISPR-Cas9 to delete *Fam134B* (Fregno *et al*, 2018) transfected with an empty pcDNA3 plasmid.

C Same as (B) in cells back-transfected with active FAM134B.

D Same as (B) in cells back-transfected with inactive FAM134B (FAM134BLIR), which cannot bind LC3.

E Quantification of HA-positive endolysosomes (B-D) (mean, $n = 17$, 13 and 10). One-way ANOVA and Dunnett's multiple comparison test, ns $P > 0.05$, ****$P < 0.0001$.

F HEK293 cells transfected with empty vector (lane 1), ATZ-HA (2), FAM134B-V5 (3), FAM134B-V5 and ATZ-HA (4), or FAM134BLIR-V5 and ATZ-HA (5), treated for 6 h with 100 nM BafA1 and then cross-linked with DSP before lysis (see Materials and Methods). FAM134BLIR-V5 interacts with CNX and ATZ-HA, but not with LC3.

G–I (G) Same as (B) in control CRISPR cells and (H) in cells edited with CRISPR/Cas9 to delete *Sec62* (Fumagalli *et al*, 2016) or (I) *Tex264*.

J, K (J) Quantification of (G–I) for HA-positive endolysosomes, (mean, $n = 11$, 11, 22) and (K) for 2C1-positive endolysosomes (mean, $n = 11$, 9, 11). One-way ANOVA and Dunnett's multiple comparison test, ns $P > 0.05$.

Data information: Scale bars 10 μm.
Source data are available online for this figure.

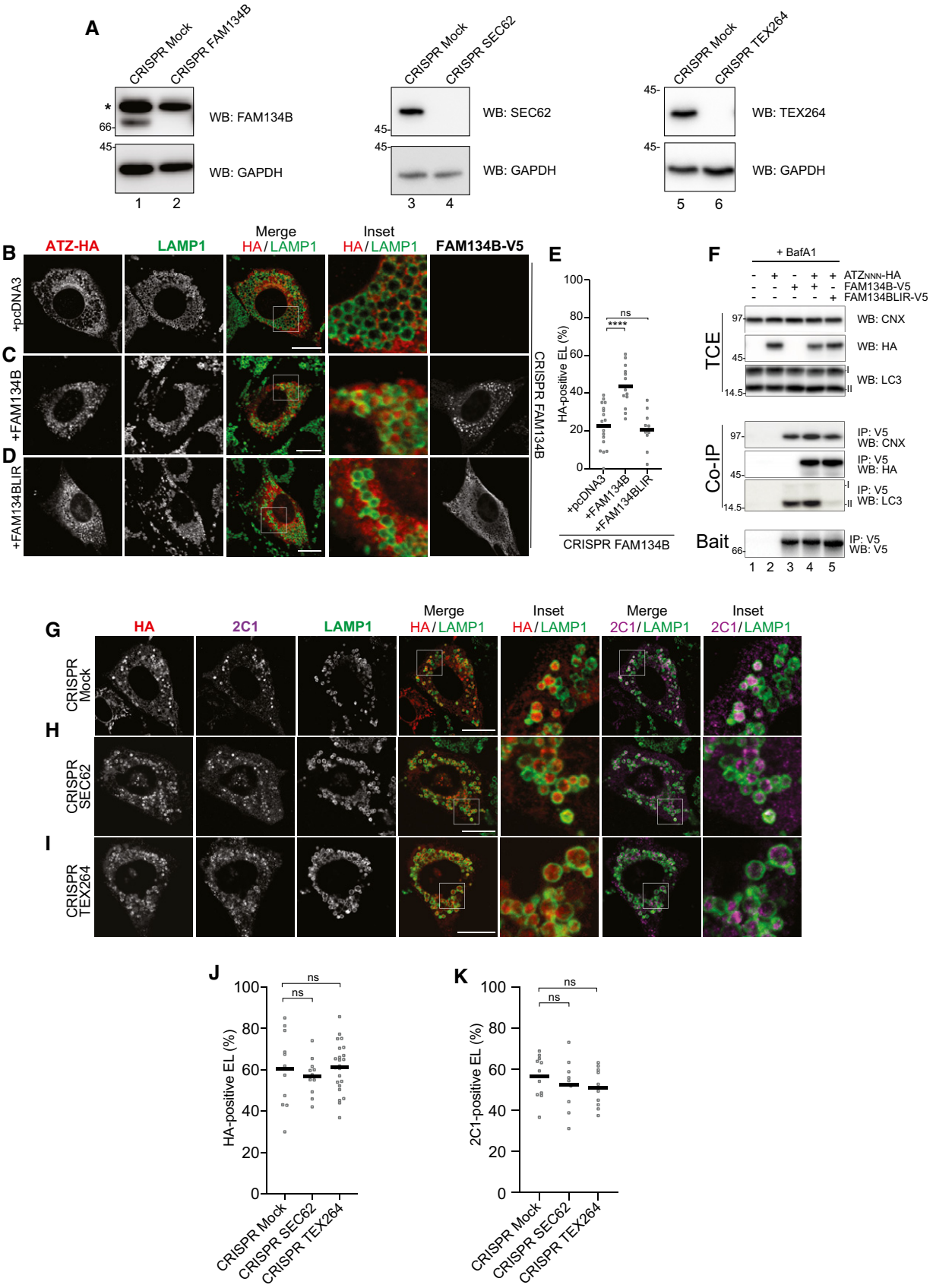
A
CRISPR Mock
CRISPR FAM134B
WB: FAM134B
WB: GAPDH
CRISPR SEC62
WB: SEC62
CRISPR TEX264
WB: TEX264
B
ATZ-HA
LAMP1
Merge HA/LAMP1
Inset HA/LAMP1
FAM134B-V5
+pcDNA3
+FAM134B
+FAM134BLIR
CRISPR FAM134B
C
D
E
HA-positive EL (%)
ns
****
CRISPR FAM134B
F
+ BafA1
ATZNNN-HA
FAM134B-V5
FAM134BLIR-V5
TCE
WB: CNX
WB: HA
WB: LC3
Co-IP
IP: V5 WB: CNX
IP: V5 WB: HA
IP: V5 WB: LC3
Bait
IP: V5 WB: V5
G
HA
2C1
LAMP1
Merge HA/LAMP1
Inset HA/LAMP1
Merge 2C1/LAMP1
Inset 2C1/LAMP1
CRISPR Mock
H
CRISPR SEC62
I
CRISPR TEX264
J
HA-positive EL (%)
K
2C1-positive EL (%)

Figure EV1.

Figure EV2. Control of polymerization propensity.

A Flow cytometric analyses of intracellular ATZ_{NNN} detected with anti-HA (*X*-axis) and anti-2C1 antibody (*Y*-axis). Cells containing ATZ_{NNN} polymers are in the upper right quadrant being immunoreactive to both anti-HA and 2C1 antibody. Analyses have been performed for the conditions and cell lines shown in Fig 2A–G.

B Control of polymerization propensity for the ATZ_{NNN} in WT (lanes 1, 2), *Uggt1*-KO (lane 3), and *Cnx*-KO MEF (lane 4). Polymers and monomers are seen with anti-HA (upper panel) or with the polymer-specific 2C1 antibody (middle panel). Total protein in SDS-polyacrylamide gels in lower panel.

C Same as (A) for cells expressing glycosylation mutants as in Fig 3B–I.

D Same as (B) for the 4 glycosylation mutants shown in Fig 4, for AAT and for the non-polymerogenic, disease-causing NHK variant of AAT expressed in HEK293 cells.

Source data are available online for this figure.

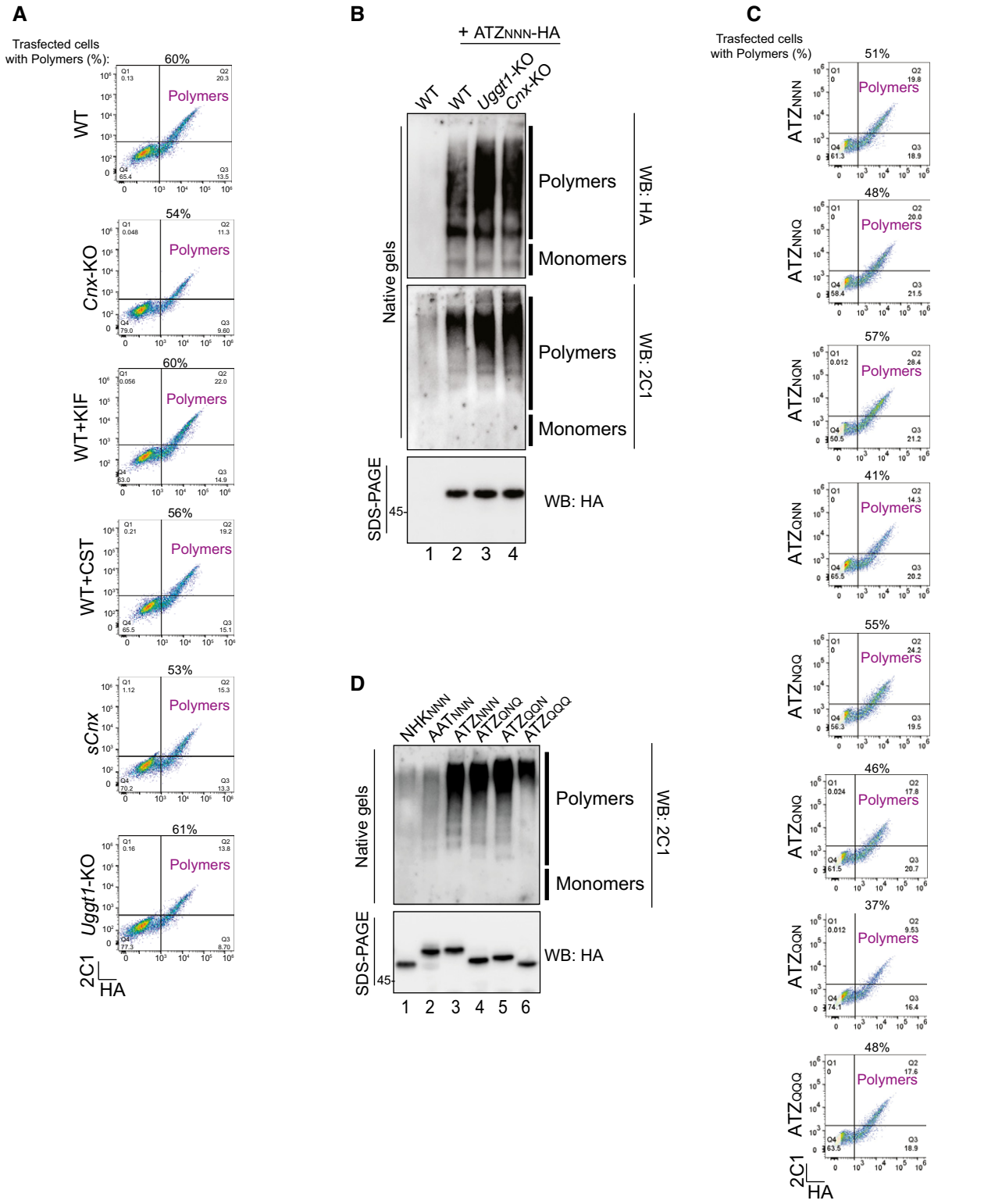
A
Trasfected cells with Polymers (%):
WT
60%
Cnx-KO
54%
WT+KIF
60%
WT+CST
56%
sCnx
53%
Uggt1-KO
61%
Polymers
2C1
HA
B
+ ATZNNN-HA
WT
WT
Uggt1-KO
Cnx-KO
Native gels
Polymers
Monomers
WB: HA
WB: 2C1
SDS-PAGE
45-
WB: HA
1 2 3 4
C
Trasfected cells with Polymers (%)
ATZNNN
51%
ATZNNQ
48%
ATZNQN
57%
ATZQNN
41%
ATZNQQ
55%
ATZQNQ
46%
ATZQQN
37%
ATZQQQ
48%
Polymers
2C1
HA
D
NHKNNN
AATNNN
ATZNNN
ATZQNQ
ATZQQN
ATZQQQ
Native gels
Polymers
Monomers
WB: 2C1
SDS-PAGE
45-
WB: HA
1 2 3 4 5 6

Figure EV2.

Figure EV3. Requirements for endolysosomal delivery of Pro-collagens.

A Schematic representation of glycosylated Pro-Col2A1$_{(WT)}$N and Pro-Col2A1$_{(R989C)}$N and of non-glycosylated Pro-Col2A1$_{(WT)}$Q and Pro-Col2A1$_{(R989C)}$Q (N-glycan in red, mutation in blue).

B–E Confocal laser scanning microscopy analyses as in Fig 2, for Pro-Col2A1($_{WT}$)N/Q and Pro-Col2A1(R_{989}C)N/Q.

F Quantification of Pro-collagen-positive endolysosomes (B–E) (mean, n = 21, 35, 13 and 15 cells). One-way ANOVA and Dunnett's multiple comparison test, ****$P < 0.0001$.

G Same as (D).

H Same as (G) in *Cnx*-KO cells.

I Same as (G) in kifunensine (KIF)-treated cells.

J Same as (G) in castanospermine (CST)-treated cells.

K Same as (G) in sCnx cells.

L Same as (G) in *Uggt1*-KO cells.

M Quantification of (G–L) (mean, n = 23, 12, 17, 20, 12 and 18 cells). One-way ANOVA and Dunnett's multiple comparison test, ns $P > 0.05$, ***$P < 0.001$, ****$P < 0.0001$.

Data information: Scale bars 10 μm.

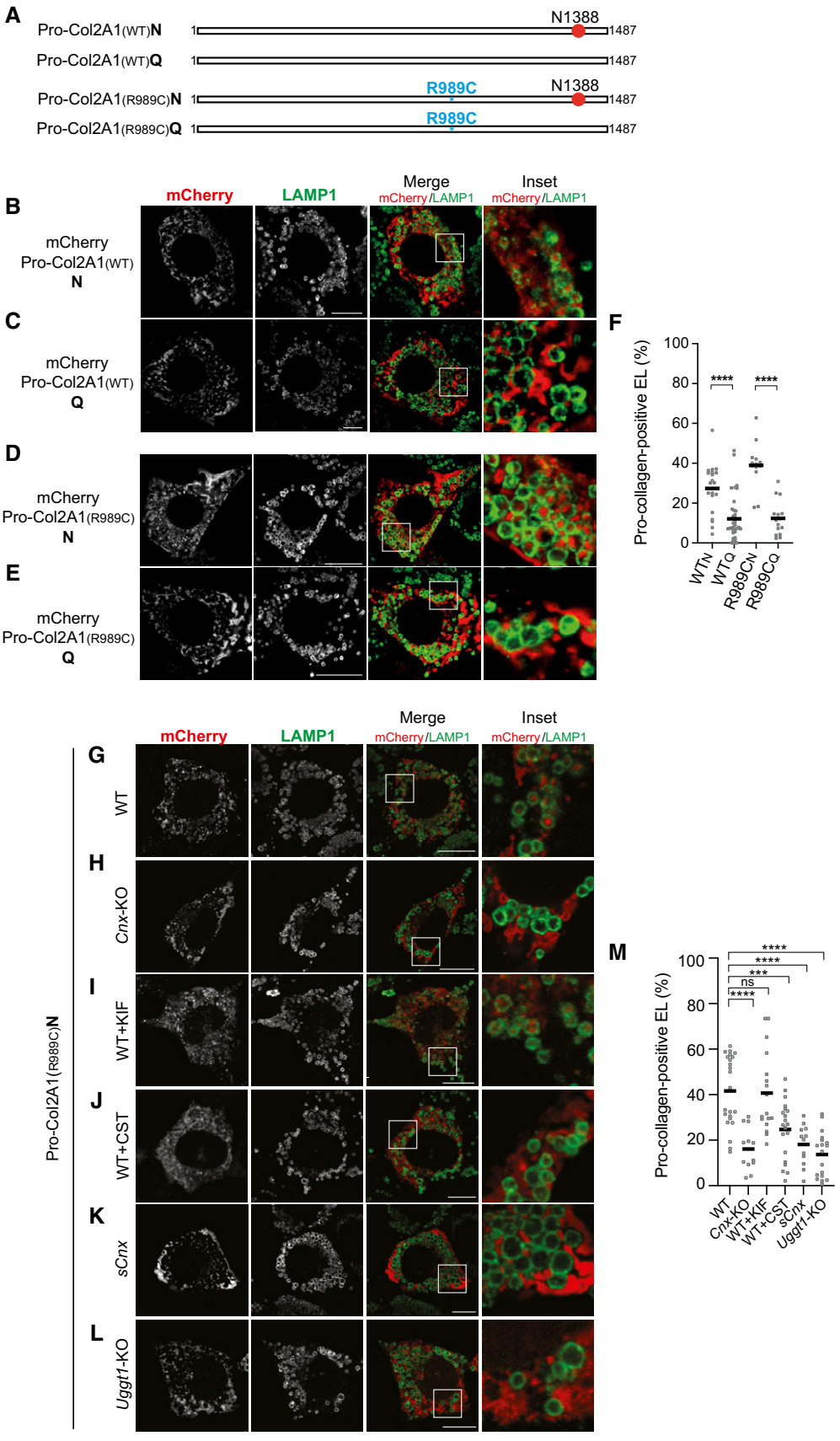
A
Pro-Col2A1(WT)N
Pro-Col2A1(WT)Q
Pro-Col2A1(R989C)N
Pro-Col2A1(R989C)Q
N1388
R989C
1
1487
B
C
D
E
mCherry
LAMP1
Merge
mCherry/LAMP1
Inset
mCherry/LAMP1
mCherry Pro-Col2A1(WT) N
mCherry Pro-Col2A1(WT) Q
mCherry Pro-Col2A1(R989C) N
mCherry Pro-Col2A1(R989C) Q
F
Pro-collagen-positive EL (%)
WTN
WTQ
R989CN
R989CQ
****
Pro-Col2A1(R989C)N
G WT
H Cnx-KO
I WT+KIF
J WT+CST
K sCnx
L Uggt1-KO
M
ns
***
WT
Cnx-KO
WT+KIF
WT+CST
sCnx
Uggt1-KO

Figure EV3.

Figure EV4. FAM134B:CNX:ATZ$_{NNN}$ complexes and intracellular localization of ATZ polymers.

A Same as EV1F in WT and sCNX MEF, without DSP.
B Same as (A) in WT and *Uggt1*-KO MEF.
C Same as Fig 2A with the endolysosomal marker LAMP1 and the ER marker CLIMP63.
D Same as (C) for *Cnx*-KO.
E Same as (C) for *Uggt1*-KO.
F–H HaloTag pulse-chase analysis in WT, *Cnx*-KO, and *Uggt1*-KO MEF monitoring fluorescent Halo-ATZ$_{NNN}$ generated during a 45 min pulse with JF646, at 6 h of chase in the absence of BafA1. Arrowheads show select clusters of JF646-labeled Halo-ATZ$_{NNN}$ co-localizing with BiP.
I Analyses of soluble and insoluble ATZ$_{NNN}$ in WT, *Cnx*-KO, and *Uggt1*-KO MEF.

Data information: Scale bars 10 μm.
Source data are available online for this figure.

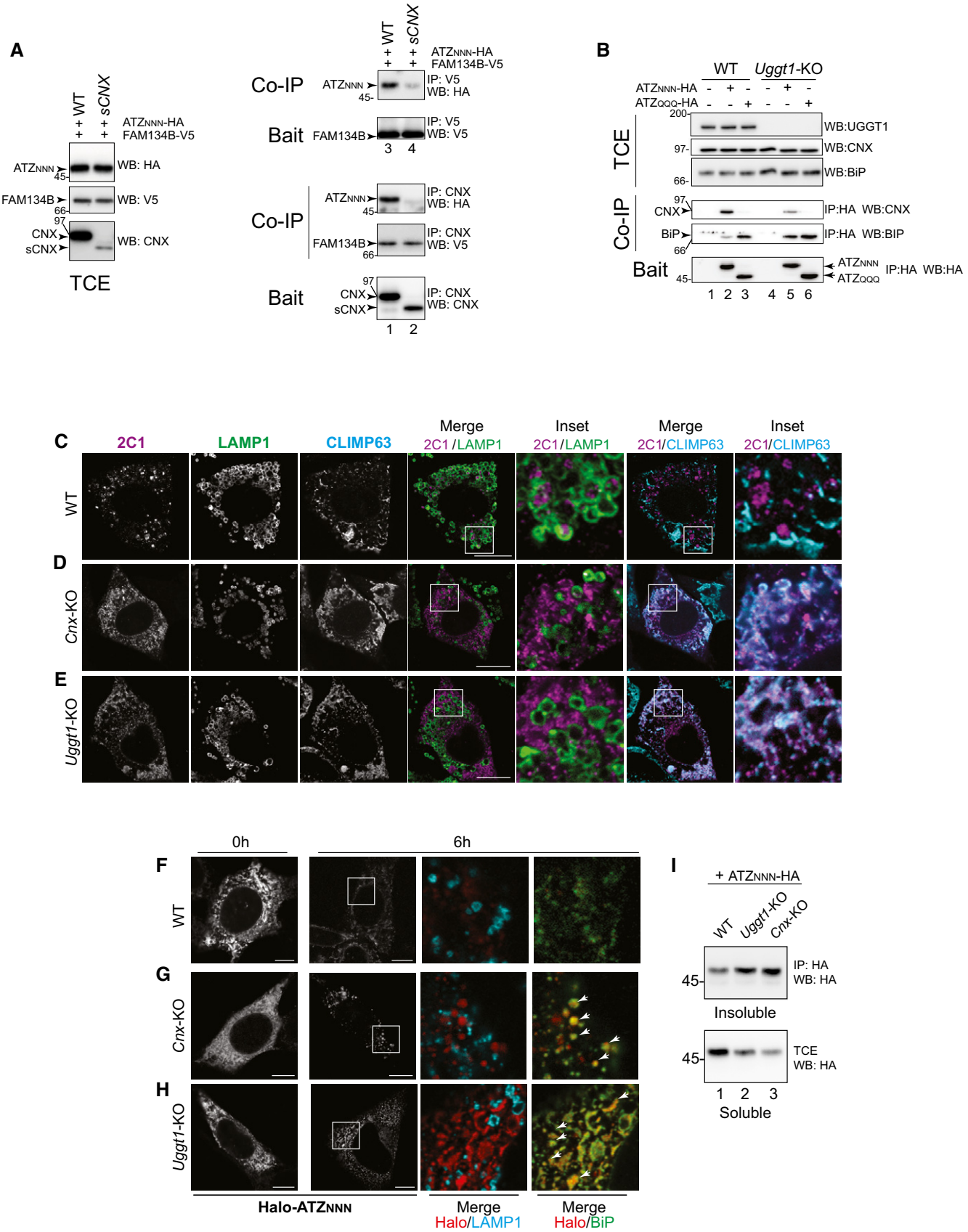
A
+ WT
+ sCNX
ATZNNN-HA
FAM134B-V5
ATZNNN
WB: HA
FAM134B
WB: V5
CNX
sCNX
WB: CNX
TCE
Co-IP
Bait
IP: V5
IP: CNX
B
WT
Uggt1-KO
ATZNNN-HA
ATZQQQ-HA
WB:UGGT1
WB:CNX
WB:BiP
IP:HA WB:CNX
IP:HA WB:BIP
IP:HA WB:HA
C
2C1
LAMP1
CLIMP63
Merge 2C1/LAMP1
Inset 2C1/LAMP1
Merge 2C1/CLIMP63
Inset 2C1/CLIMP63
WT
D
Cnx-KO
E
Uggt1-KO
F
0h
6h
G
H
Halo-ATZNNN
Merge Halo/LAMP1
Merge Halo/BiP
I
+ ATZNNN-HA
Insoluble
Soluble
IP: HA
WB: HA
TCE

Figure EV4.

Figure EV5. Delivery of ATZ_{xxx} within endolysosomes in human, mouse, and hamster cell lines.

A–D Same as Fig 3 in HEK293 cells. Endolysosomes are labeled with GFP-RAB7.
E Quantification of HA-positive endolysosomes (A-D) (mean, $n = 18, 16, 16, 15$ cells).
F–I Same as Fig 3 in HEPA1-6 cells.
J Quantification of (F–I) (mean, $n = 13, 12, 12, 13$ cells).
K–N Same as Fig 3 in HeLa cells.
O (J) Quantification of (K–N) (mean, $n = 16, 11, 14, 14$ cells).
P Same as Fig 3 in CHO cells. The polymer-specific 2C1 antibody stain is shown.

Data information: One-way ANOVA and Dunnett's multiple comparison test, ns $P > 0.05$, ****$P < 0.0001$. Scale bars 10 μm.

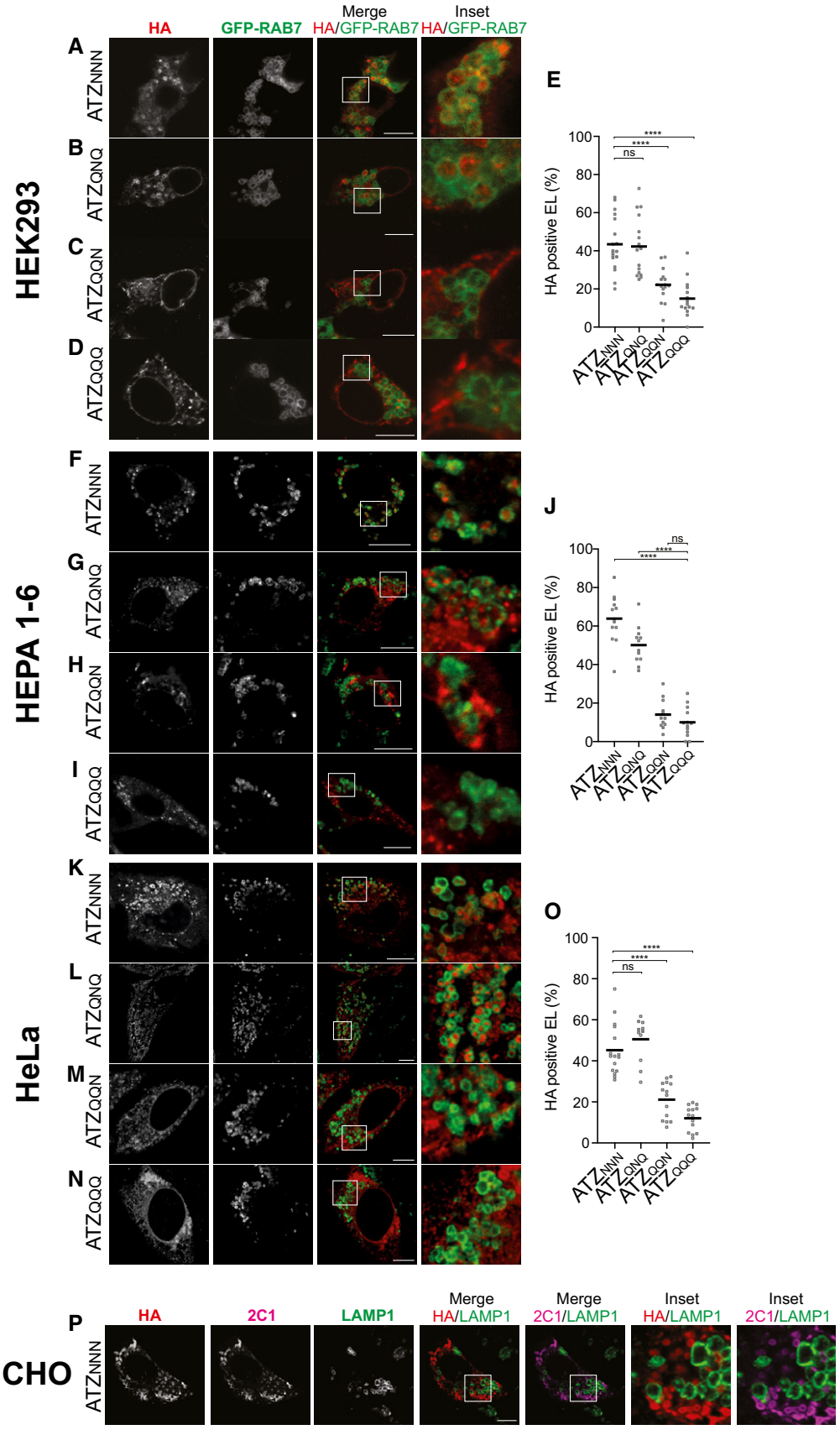
HA
GFP-RAB7
Merge HA/GFP-RAB7
Inset HA/GFP-RAB7
HEK293
HEPA 1-6
HeLa
CHO
A ATZNNN
B ATZQNQ
C ATZQQN
D ATZQQQ
E
F ATZNNN
G ATZQNQ
H ATZQQN
I ATZQQQ
J
K ATZNNN
L ATZQNQ
M ATZQQN
N ATZQQQ
O
HA positive EL (%)
ns
****
P ATZNNN
2C1
LAMP1
Merge HA/LAMP1
Merge 2C1/LAMP1
Inset HA/LAMP1
Inset 2C1/LAMP1

Figure EV5.